Q_α values in superheavy nuclei from the deformed Woods-Saxon model

P. Jachimowicz
Institute of Physics, University of Zielona Góra, Szafrana 4a, 65516 Zielona Góra, Poland

M. Kowal* and J. Skalski
National Centre for Nuclear Research, Hoża 69, PL-00-681 Warsaw, Poland
(Received 26 November 2013; published 5 February 2014)

Masses of superheavy (SH) nuclei with $Z = 98$–128, including odd and odd-odd nuclei, are systematically calculated within the microscopic-macroscopic model based on the deformed Woods-Saxon potential. Ground states are found by minimizing energy over deformations and configurations. Pairing in odd particle-number systems is treated either by blocking or by adding the BCS energy of the odd quasiparticle. Three new parameters are introduced which may be interpreted as the constant mean pairing energies for even-odd, odd-even, and odd-odd nuclei. They are adjusted by a fit to masses of heavy nuclei. Other parameters of the model, fixed previously by fitting masses of even-even heavy nuclei, are kept unchanged. With this adjustment, the masses of SH nuclei are predicted and then used to calculate α-decay energies to be compared to known measured values. It turns out that the agreement between calculated Q_α values with data in SH nuclei is better than in the region of the mass fit. The model overestimates Q_α for $Z = 111$–113. Ground state (g.s.) configurations in some SH nuclei hint to a possible α-decay hindrance. The calculated configuration-preserving transition energies show that in some cases this might explain discrepancies, but more data are needed to explain the situation.

DOI: 10.1103/PhysRevC.89.024304 PACS number(s): 21.10.Dr, 23.60.+e, 25.70.Jj, 27.90.+b

I. INTRODUCTION

Most of the currently known heaviest nuclei, in particular all beyond $Z = 114$, decay via a sequence of α particle emissions [1–7]. Energy release in an α decay of a nucleus with Z protons and N neutrons, $Q_\alpha(Z,N)$, is directly related to nuclear masses

$$Q_\alpha(Z,N) = M(Z,N) - M(Z-2,N-2) - M(2,2). \quad (1)$$

Hence energies E_α[1] measured in a chain of α decays provide a link between masses of parent and daughter nuclei if they can be identified as g.s. to g.s. transitions. They can also determine a newly created nuclide when E_α of one of the consecutive decays matches the value characteristic of an already known parent isotope. Besides providing a hint for the identification of new elements, Q_α values are the main factor determining the half-life with respect to the α decay. Since these half-lives directly relate to the detection pattern, a possibly accurate determination of Q_α is important for the search for new elements. Finally, although many masses of SH isotopes are unknown, this observable provides a test of a local dependence of theoretical masses on Z and N.

While the calculations of masses for even-even nuclei are readily available in the literature, similar systematic calculations for the odd and odd-odd systems are less frequent. Here, we report such calculations for heavy and SH nuclei within the microscopic-macroscopic model based on the deformed Woods-Saxon potential [8]. This model was widely applied to many problems of nuclear structure over many years. Recently, in a version adjusted to heavy nuclei [9], we used it to reproduce data on first [10], second [11], and third barriers [12,13] and on second minima [14] in actinides and to predict ground states and saddle points in superheavy nuclei up to $Z = 126$ [15]. The general motivation of our study is to sharpen predictions of the model, i.e., masses, Q_α values and fission barriers, by accounting for sufficiently many deformations (which, for technical reasons, was not always practical in the past). The results obtained up to now reveal the importance of including some deformations, neglected in the previous calculations. This concerns especially studies of first, second, and third fission barriers. In the region of SH nuclei, the predicted abundance of triaxial saddle points for $Z \geqslant 120$ [15,16] calls into question all calculations assuming axial symmetry done previously.

In the present paper we continue along this line by extending our model, which up to now was applied mainly to even-even nuclei, to odd and odd-odd nuclei. To be sure, the Woods-Saxon model was used for odd SH nuclei previously, see for example [17–19]. However, there are important differences between the present study and the previous ones: a different version of macroscopic energy giving different results, more restricted equilibrium shapes and fewer nuclei were studied in [17,18]; the study of ground and excited states in [19] was performed solely without blocking.

In extending the model we prefer to keep all essential parameters fixed in [9] unchanged. The extension of the microscopic part consists in calculating the shell and pairing correction energy for a system with an odd number of nucleons. This is done in two ways, differing by a treatment of the odd particle. The macroscopic part is modified by including an additional average pairing energy contribution, different for even-odd, odd-even, and odd-odd nuclei. These contributions are chosen as constants and fixed by a fit to the masses of

*m.kowal@fuw.edu.pl

[1]The α particle energy is in direct relationship with Q value $E_\alpha = \frac{A-4}{A} Q_\alpha$ where A is the mass number.

translead nuclei known in 2003, in analogy to the fit for even-even nuclei done in [9]. After that, the ground states of 1364 nuclei, from $Z = 98$ to $Z = 128$, are determined by energy minimization over configurations with zero or one blocked particle over axially symmetric deformations. The α-decay energies of SH nuclei calculated from these masses are compared to the measured values, including recent isotopic chains for $Z = 117$ [20]. This allows to appreciate the performance of the model outside the region of the original fit and to discuss some possible structure effects. We also make comparisons with results of some other models.

A description of our model and calculations is given in Sec. II. The results are presented and discussed in Sec. III. Finally, the conclusions are summarized in Sec. IV.

II. THE MODEL

Our microscopic-macroscopic model is based on a deformed Woods-Saxon potential [8]. In this study we focus on nuclear ground states. Therefore, it is possible to confine analysis to axially symmetric shapes defined by the following equation of the nuclear surface:

$$R(\theta) = c(\{\beta\})R_0\left[1 + \sum_{\lambda=2}\beta_{\lambda 0}Y_{\lambda 0}(\theta)\right], \qquad (2)$$

where $c(\{\beta\})$ is the volume-fixing factor and R_0 is the radius of a spherical nucleus. For the macroscopic part we used the Yukawa plus exponential model [21]. With the aim of adjusting the model especially for heavy and superheavy nuclei, three parameters of the macroscopic energy formula and the pairing strengths were determined in [9] by a fit to masses of even-even nuclei with $Z \geqslant 84$ and $N > 126$ as given in [22]. These parameters were used since then in all our calculations.

For systems with odd proton or neutron (or both), a standard treatment is that of blocking. Considered configurations consist of an odd particle occupying one of the levels close to the Fermi level and the rest of the particles forming a paired BCS state on the remaining levels. The ground state is found by looking for a configuration (blocking particles on levels from the tenth below to tenth above the Fermi level) and deformation giving the energy minimum. In the present study, we used this procedure including mass-symmetric deformations $\beta_2, \beta_4, \beta_6$, and β_8, i.e., the four-dimensional minimization is performed by the gradient method and, for the check, on the mesh of deformations:

$$\begin{aligned}\beta_{20} &= -0.30\ (0.02)\ 0.32,\\ \beta_{40} &= -0.08\ (0.02)\ 0.18,\\ \beta_{60} &= -0.10\ (0.02)\ 0.12,\\ \beta_{80} &= -0.10\ (0.02)\ 0.12.\end{aligned} \qquad (3)$$

Both sets of results are consistent; lower energies from the gradient method are treated as final. The used deformation set should provide for a fair approximation, except for the region of light isotopes of elements between Rn and light actinides, which show octupole deformation in their ground states. The values of parameters from [9] were left unchanged for even-even nuclei. For the rest, we introduced three new parameters—additive constants which may be interpreted as corrections for the mean pairing energy in even-odd, odd-even, and odd-odd nuclei. These parameters were fixed by a fit to the masses of odd-even, even-odd, and odd-odd $Z \geqslant 82$ and $N > 126$ nuclei taken from [23].

It is known that the blocking procedure often causes an excessive reduction of the pairing gap in systems with odd particle number. One device to avoid an excessive even-odd staggering in nuclear binding was to assume stronger (typically by $\sim 5\%$) pairing interaction for odd-particle-number systems, see [24]. Since the main predictions of this work are Q_α values in which the effect of stronger pairing in parent and daughter nuclei partially cancels out, we postpone for the future a more elaborate treatment of this effect. Instead, we performed another calculations of nuclear masses without blocking. Shell (and pairing) correction energy of a configuration with an odd neutron (or proton) was taken as a sum of the quasiparticle energy of a singly occupied level $\sqrt{(\epsilon - \lambda)^2 + \Delta^2}$ and the shell (and pairing) correction calculated without blocking. The latter quantity, as well as the pairing gap Δ and the Fermi energy λ, are calculated for the odd number of particles, but with the double occupation of all levels. This prescription was used before in [19]. It gives results similar to those obtained when calculating Δ, λ, and the shell (and pairing) correction for the even system with one particle less. The calculation without blocking is much simpler and we were able to perform a seven-dimensional minimization over axially symmetric deformations $\beta_{20}, \beta_{30}, \beta_{40}, \beta_{50}, \beta_{60}, \beta_{70}$, and β_{80}. Therefore, these results should be reliable also for light actinides. As we preferred to avoid a new fit of the macroscopic model parameters, also for this model we introduced three additive constants (energy shifts) for even-odd, odd-even, and odd-odd nuclei which minimize the rms deviation in each of the groups of nuclei.

A. Odd-odd nuclei

Structure of odd-odd nuclei is more complicated than that of odd-A systems. If we disregard collective vibrations, the ground state configuration is a result of coupling the unpaired neutron and proton to a total angular momentum. The energy ordering of coupled configurations is usually attributed to a residual neutron-proton interaction V_{np}. In spherical nuclei it is summarized by the empirical Nordheim rule [25].

In deformed, axially symmetric nuclei, in which the projection of the single-particle angular momentum on the symmetry axis Ω is a good quantum number, the n-p coupling can give two configurations with $K = |\Omega_p \pm \Omega_n|$. According to the empirical Gallagher-Moszkowski rule [26], the one energetically favoured is the spin triplet state. The spin structure of both n and p single particle orbitals shows which K configuration will be the lower one. A collective rotational band is built on each of two bandheads. Energies of the band members with angular momentum I are usually presented as [27]

$$E(I,K) = E(n,p) + \frac{\hbar^2}{2\mathcal{J}}[I(I+1) - K^2] + E_K + (-)^I\delta_{K,0}(E_0 + E_a), \qquad (4)$$

TABLE I. Statistical parameters of the fit to masses in the model with blocking in separate groups of even-even, odd-even, even-odd, and odd-odd heavy nuclei: the number N of nuclei in the group, the energy shift h, the average discrepancy $\langle|M^{\rm exp} - M^{\rm th}|\rangle$, the maximal difference $\max|M^{\rm exp} - M^{\rm th}_f|$, the rms deviation $\delta_{\rm rms}$. Experimental data taken from [23]. All quantities are in MeV, except for the number of nuclei N.

N	e-e 74	o-e 56	e-o 69	o-o 53
h	0.000	1.013	0.824	1.703
$\langle\|M^{\rm th} - M^{\rm exp}\|\rangle$	0.212	0.340	0.356	0.566
$\max\|M^{\rm th} - M^{\rm exp}\|$	0.833	0.836	1.124	1.387
$\delta_{\rm rms}$	0.284	0.425	0.435	0.666

where $E(n,p)$ represents the mean-field energy of a band-head configuration, the second term is the rotational energy, E_K is the diagonal matrix element of V_{np}, the last term, combined of the Newby shift E_0 and the diagonal Coriolis term E_a for $\Omega_n = \Omega_p = 1/2$, occurs only for $K = 0$ bands and splits them into two sub-bands. In such a formula, all off-diagonal matrix elements of the interaction V_{np} and of the rotor-plus-two-particles Hamiltonian are neglected. From the experimental data in rare earth and actinide regions, the Newby shifts E_0 and Gallagher-Moszkowski shifts, defined as $\Delta E_{\rm GM} = E_{K<} - E_{K>} = \hbar^2\Omega_</\mathcal{J} + E_{\rm bh}(K_<) - E_{\rm bh}(K_>)$, were extracted [27,28]. The former are usually less than 50 keV, while the latter amount to 100–300 keV.

The above information is incorporated in mass formulas by defining some average (i.e., configuration-independent) neutron-proton energies for odd-odd nuclei. Their role is to account for the shift in the g.s. energy with respect to the value calculated with blocking or quasiparticle method that would simulate on average the terms beyond $E(n,p)$ in Eq. (4). For example, in [29], the additional binding δ_{np} is included which amounts to ~200 keV for odd-odd actinides. Although this term is A dependent in [29], one can see that the difference in it between actinides and superheavy nuclei is around 20 keV. Therefore, as we confine here our model to heavy and superheavy nuclei, we assume constant average neutron-proton and average pairing energies. This leaves three constants: $h_{\rm oe}$, $h_{\rm eo}$, and $h_{\rm oo}$ (see Tables I and II) that can be fit to odd-A and odd-odd nuclei; they correspond to the parameters $\bar{\Delta}_n$, $\bar{\Delta}_p$, and $\bar{\Delta}_n + \bar{\Delta}_p - \delta_{np}$ of the model used in [29]. Thus, we calculate the mass of an odd-odd nucleus within the blocking method by adding 1.703 MeV to the micro-macro energy of the optimal configuration. This corresponds to the neutron-proton energy of $h_{\rm oe} + h_{\rm eo} - h_{\rm oo} = 134$ keV (Table I).

TABLE II. The same as in Table I but for the method without blocking.

N	e-e 74	o-e 56	e-o 69	o-o 53
h	0.000	−0.751	0.268	0.234
$\langle\|M^{\rm th} - M^{\rm exp}\|\rangle$	0.187	0.460	0.273	0.295
$\max\|M^{\rm th} - M^{\rm exp}\|$	0.652	1.398	0.892	0.853
$\delta_{\rm rms}$	0.251	0.551	0.343	0.366

Since the g.s. configurations must be energetically favored, the parent and daughter energy shifts E_K will cancel in large part in Q_α values.

B. Configuration hindrance of α transitions

Considering a comparison of measured and calculated α-decay energies, it is important to observe the hindrance of α transitions between different configurations in odd-A and odd-odd nuclei. Although a degree of this hindrance is surely configuration-dependent, if strong enough, it can hide the true Q_α value when only a few transitions are detected in experiment. At present, this is the situation in many heaviest nuclei.

One can consult the known data to see the magnitude of hindrance. For example, the isotopes ^{251}Fm, ^{253}No, and ^{255}Rf decay primarily to the $9/2^-$ parent g.s. configurations in daughters, which lie at the excitation energy of 200–400 keV, with probabilities, respectively, 87% [30], 96% [31], and >90% [32]. In 82% of cases, ^{249}Cf decays to the $9/2^-$ parent configuration; the $7/2^+$ g.s. in ^{245}Cm daughter is populated only in 2.5% of cases [33]. In the decay of ^{251}Cf, the hindrance of the g.s. to g.s. transition ($1/2^+ \to 9/2^-$) results in the g.s. band in daughter receiving ~15% of cases; 2.6% of those decays goes to the g.s. [34]. Much reduced K-hindrance is seen in the decay of ^{249}Bk ($7/2^+$): more than 90% of decays goes to the g.s. rotational band in ^{245}Am, built on the $5/2^+$ configuration, in that 6.6% to the g.s. [35].

Motivated by these examples, to set an upper limit for an underestimate of Q_α, we also calculate apparent Q_α values taking the parent g.s. configuration as the final state in daughter. Such a value is smaller than the true Q_α by the excitation of the parent g.s. configuration in the daughter. Gallagher shifts also mostly cancel in such transition energies.

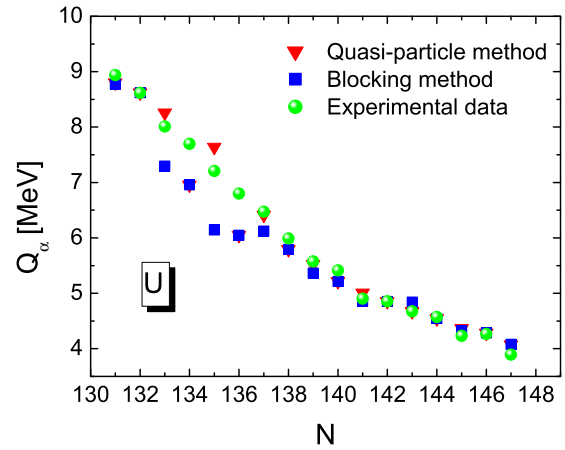

FIG. 1. (Color online) Q_α values for U ($Z = 92$) nuclei: circles—experiment, squares—model with blocking, triangles—model without blocking.

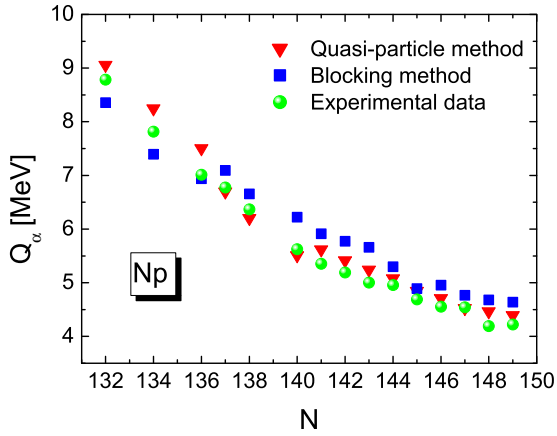

FIG. 2. (Color online) As in Fig. 1, but for Np ($Z = 93$) isotopes.

III. RESULTS AND DISCUSSION

The quality of the mass fit is summarized in Tables I and II where the deviations from the experimental masses are given for each of the four groups of nuclei. The data are taken from [23], also for even-even nuclei. Statistical parameters of the fit for this group are different in Tables I and II because of different deformations included. Deviations in Table II slightly differ from those in [9] because we used here a larger number of data from [23]. One can observe that the model with blocking is worse for even-odd and odd-even systems than for the even-even ones; the quality deteriorates further for odd-odd systems. A different situation occurs for the results without blocking: the worst case are the odd-even systems; odd-odd masses are rather well described. The differences in $\delta_{\rm rms}$ between groups of nuclei may show a need to refit some of the parameters fixed for even-even nuclei, but this requires more study.

One can observe that our local fit is better that those resulting from the self-consistent models. For example, after adding to the typical Skyrme forces the phenomenological Wigner term, microscopic contact pairing force and correction for spurious collective energy, the root-mean square deviation equal 0.58 MeV has been obtained in a global calculation, see Refs. [36,37]. In another Hartree-Fock-Bogoliubov (HFB) model [38], aimed at fitting simultaneously masses and fission data, a phenomenological correction for collective vibrations allowed to obtain the rms deviation of 0.729 MeV. Recently HFB calculations via refitting to the 2012 Atomic Mass Evaluation (AME) and varying the symmetry coefficients gave in the best case a value of 0.54 MeV rms [39].

Macroscopic-microscopic global calculations of nuclear masses made by Moller and co-workers [29] give the rms error 0.669 MeV for nuclei ranging from oxygen to hassium and 0.448 MeV in the case of nuclei above $N = 65$. A phenomenological formula with the 10 free parameters by Duflo and Zuker [40,41] gives mass estimates with the 0.574 MeV rms error. Recently, authors of [42] achieved the rms deviation of 0.34 keV in a fit to masses of 2149 nuclei, however, at the cost of including many corrections with often a rather obscure physical meaning.

The calculated and measured Q_α values for U and Np isotopes are shown in Figs. 1 and 2. They illustrate the quality of the model for nuclei from the region of the fit. We did not choose the best cases; on the contrary, the values

TABLE III. Effect of octupole deformations within blocking method.

	$M^{\rm th}$	β_{20}	β_{30}	β_{40}	β_{50}	β_{60}	β_{70}	β_{80}
^{225}U	25.490	0.134	0.123	0.074	0.045	0.012	0.011	−0.004
^{225}U	26.081	0.157	–	0.107	–	0.044	–	−0.009
^{221}Th	14.878	0.110	0.092	0.073	0.045	0.022	0.028	−0.001
^{221}Th	16.387	0.110	–	0.083	–	0.039	–	−0.022

TABLE IV. Effect of octupole deformations within quasiparticle method.

	$M^{\rm th}$	β_{20}	β_{30}	β_{40}	β_{50}	β_{60}	β_{70}	β_{80}
^{225}U	26.463	0.131	0.114	0.074	0.044	0.014	0.015	−0.003
^{225}U	27.278	0.151	–	0.103	–	0.039	–	−0.015
^{221}Th	15.778	0.103	0.093	0.069	0.047	0.021	0.030	−0.002
^{221}Th	17.247	0.104	–	0.077	–	0.038	–	−0.012

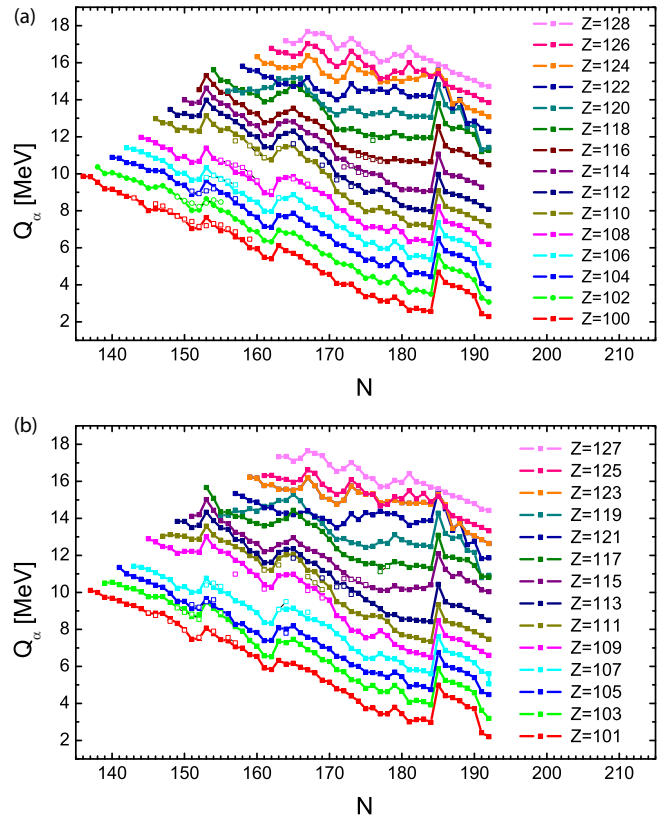

FIG. 3. (Color online) Q_α values calculated with blocking vs experimental data. Explicit values, including the source for the experimental data, are given in Table V.

TABLE V. Results of the calculations with blocking. In successive columns are given: proton number Z, neutron number N, mass number A, parent quadrupole deformation β_{20}, experimental value $Q_\alpha^{\rm exp}$ from [43], [6,20] (O), [7] (R) and [44] (*), calculated g.s. to g.s. values Q_α(g.s. $\rightarrow$ g.s.), the parent g.s. configuration $\pi\{\Omega\}_P$(g.s.) specified by the parity and Ω-quantum numbers (multiplied by 2, P—protons, N—neutrons), the daughter g.s. configuration $\pi\{\Omega\}_D$(g.s.) and the calculated decay energy $Q_\alpha(\pi\{\Omega\}_P = \pi\{\Omega\}_D)$ for the configuration-preserving transition.

Z	N	A	β_{20}	$Q_\alpha^{\rm exp}$	Q_α(g.s. $\rightarrow$ g.s.)	$\pi\{\Omega\}_P$(g.s.)		$\pi\{\Omega\}_D$(g.s.)		$Q_\alpha(\pi\{\Omega\}_P = \pi\{\Omega\}_D)$
						P	N	P	N	
119	178	297	−0.10		12.64	−1		−3		12.57
118	176	294	−0.09	11.81	12.09					
117	177	294	−0.09	11.12^O	11.32	−3	1	−5	1	11.25
117	176	293	−0.09	11.36^O	11.53	−3		−5		11.45
116	177	293	−0.08	10.68	10.80		1		1	10.80
116	176	292	−0.08	10.77	10.92					
116	175	291	0.08	10.89	11.01		1		5	10.89
116	174	290	−0.09	10.99	11.14					
115	175	290	−0.08	10.42^O	10.41	−5	1	−7	5	10.11
115	174	289	−0.09	10.69^O	10.60	−5		−3		10.56
115	173	288	0.08	10.70^R	10.76	−1	5	−3	5	10.54
115	172	287	−0.11	10.74	11.01	−5		−3		10.61
114	175	289	0.09	9.97	10.00		1		−15	9.93
114	174	288	0.09	10.07	10.32					
114	173	287	0.09	10.16	10.44		5		5	10.44
114	172	286	−0.12	10.37	10.80					
113	173	286	0.09	9.89^O	10.13	−7	5	−1	5	9.68
113	172	285	0.14	10.33^O	10.45	−3		11		10.27
113	171	284	0.14	10.30^R	10.52	−3	5	−9	5	10.34
113	170	283	0.15		11.09	−3		−3		11.09
113	169	282	0.21	10.78	11.22	−1	1	−3	5	10.71
113	168	281	0.21		11.56	−1		−3		11.34
113	167	280	0.21		11.60	−1	5	−3	3	11.25
113	166	279	0.21		12.02	−1		−3		11.81
113	165	278	0.21	11.85	12.33	−1	3	−3	−13	11.56
112	173	285	0.11	9.32	9.48		−15		5	9.35
112	172	284	0.13		9.77					
112	171	283	0.13	9.67*	9.91		5		9	9.91
112	170	282	0.14		10.69					
112	169	281	0.20	10.46	11.07		1		5	10.78
112	168	280	0.19		11.38					
112	167	279	0.20		11.45		5		3	11.31
112	166	278	0.20		11.86					
112	165	277	0.21	11.62	12.21		3		−13	11.66
111	171	282	0.14		9.49	−1	5	11	9	9.24
111	170	281	0.15		10.36	11		11		10.36
111	169	280	0.16	10.15^R	10.77	−9	5	11	5	10.03
111	168	279	0.20	10.52	11.13	−3		11		10.57
111	167	278	0.21	10.85	11.18	−3	5	11	3	10.51
111	166	277	0.21		11.64	−3		11		11.11
111	165	276	0.21		11.98	−3	3	11	−13	10.95
111	164	275	0.22		12.06	−3		11		11.56
111	163	274	0.22	11.48	11.91	−3	−13	11	9	10.60
111	162	273	0.23		11.23	−3		11		10.73
111	161	272	0.23	11.20	11.28	−3	7	11	9	10.76
110	169	279	0.18		10.19		9		5	10.03
110	163	273	0.22	11.37	11.49		−13		9	10.52
110	162	272	0.23		10.75					
110	161	271	0.23	10.87	10.80		9		7	10.77
110	160	270	0.23	11.12	11.38					
110	159	269	0.23	11.51	11.61		9		−11	11.44
110	158	268	0.23		11.94					
110	157	267	0.24	11.78	12.11		3		1	12.10

TABLE V. (*Continued*).

Z	N	A	β_{20}	$Q_\alpha^{\exp}$	Q_α(g.s. $\rightarrow$ g.s.)	$\pi\{\Omega\}_P$(g.s.)		$\pi\{\Omega\}_D$(g.s.)		$Q_\alpha(\pi\{\Omega\}_P = \pi\{\Omega\}_D)$
						P	N	P	N	
109	169	278	0.19	9.69^O	9.78	11	9	−1	5	9.27
109	167	276	0.21	10.10^R	10.17	11	5	−5	3	9.46
109	166	275	0.21		10.67	11		−5		9.79
109	165	274	0.21		11.01	11	3	−5	−13	9.63
109	164	273	0.22		11.11	11		−5		9.98
109	163	272	0.22		11.02	11	−13	−5	9	9.03
109	162	271	0.23		10.27	11		−5		9.00
109	161	270	0.23	10.18	10.33	11	9	−5	7	9.01
109	160	269	0.23		10.95	11		−5		9.58
109	159	268	0.23		11.18	11	9	−5	−11	9.62
109	158	267	0.23		11.56	11		−5		10.17
109	157	266	0.24	11.00	11.73	11	3	−5	1	10.32
108	167	275	0.21	9.44	9.26		5		3	9.12
108	166	274	0.22		9.55					
108	165	273	0.22	9.73	9.89		3		−13	9.44
108	164	272	0.23		9.80					
108	163	271	0.23		9.72		−13		9	8.72
108	162	270	0.23	9.05	8.87					
108	161	269	0.24		8.91		9		7	8.82
108	160	268	0.24	9.62	9.51					
108	159	267	0.24	10.04	9.75		7		−11	9.63
108	158	266	0.24	10.35	10.04					
108	157	265	0.25	10.47	10.17		−11		3	10.15
108	156	264	0.24	10.59	10.58					
108	155	263	0.25	10.73	10.67		1		1	10.67
107	167	274	0.21	8.93	8.61	−1	5	−5	3	8.44
107	166	273	0.22		8.83	−5		9		8.79
107	165	272	0.22		9.16	−5	3	9	−13	8.71
107	164	271	0.23	9.49	9.10	−5		9		8.96
107	163	270	0.23	9.06	9.09	−5	−13	9	9	7.92
107	162	269	0.23		8.26	−5		9		7.93
107	161	268	0.24		8.33	−5	9	9	7	7.87
107	160	267	0.24		8.92	−5		9		8.45
107	159	266	0.24		9.15	−5	7	9	−11	8.56
107	158	265	0.24		9.45	−5		9		8.93
107	157	264	0.25		9.57	−5	−11	9	3	9.00
107	156	263	0.25		9.99	−5		9		9.44
107	155	262	0.25	10.32	10.11	−5	1	9	1	9.54
107	154	261	0.24	10.50	10.43	−5		9		9.89
107	153	260	0.25	10.40	10.88	−5	1	9	−9	9.68
106	165	271	0.22		8.83		3		−13	8.42
106	163	269	0.22	8.70	8.75		−13		9	7.79
106	162	268	0.23		7.89					
106	161	267	0.24		7.91		9		7	7.84
106	160	266	0.24		8.43					
106	159	265	0.25		8.62		7		−11	8.51
106	158	264	0.25		8.92					
106	157	263	0.25	9.40	9.02		−11		3	8.98
106	156	262	0.25	9.60	9.49					
106	155	261	0.25	9.71	9.60		3		1	9.52
106	154	260	0.25	9.90	9.95					
106	153	259	0.25	9.80	10.35		1		−9	9.57
105	158	263	0.25		8.26	9		−7		8.17
105	157	262	0.25		8.33	9	−11	−7	3	8.23
105	156	261	0.25		8.85	9		−7		8.73
105	155	260	0.25		8.94	9	3	−7	1	8.81
105	154	259	0.25	9.62	9.32	9		−7		9.18

TABLE V. (*Continued*).

Z	N	A	β_{20}	$Q_\alpha^{\exp}$	Q_α(g.s. $\rightarrow$ g.s.)	$\pi\{\Omega\}_P$(g.s.)		$\pi\{\Omega\}_D$(g.s.)		$Q_\alpha(\pi\{\Omega\}_P = \pi\{\Omega\}_D)$
						P	N	P	N	
105	153	258	0.25	9.50	9.72	9	1	−7	−9	8.75
105	152	257	0.25	9.21	9.03	9		−7		8.83
105	151	256	0.25	9.34	8.98	9	−9	−7	7	8.74
104	159	263	0.24		7.85		7		−11	7.74
104	157	261	0.25	8.65	8.37		−11		3	8.30
104	156	260	0.25		8.83					
104	155	259	0.25		8.97		3		1	8.87
104	154	258	0.25	9.19	9.28					
104	153	257	0.25	9.08	9.66		1		−9	8.75
104	152	256	0.25	8.93	8.93					
104	151	255	0.25	9.06	8.90		−9		7	8.83
103	157	260	0.25		8.12	−7	−11	−1	3	7.60
103	156	259	0.25		8.57	−7		−1		8.10
103	155	258	0.25	8.90	8.78	−7	3	−1	1	8.12
103	154	257	0.25		9.04	−7		−1		8.50
103	153	256	0.25		9.45	−7	1	−1	−9	8.00
103	152	255	0.25	8.56	8.70	−7		−1		8.20
103	151	254	0.25	8.82	8.65	−7	−9	−1	7	8.07
103	150	253	0.25	8.92	9.10	−7		−1		8.65
103	149	252	0.25	9.16	9.25	−7	7	−1	5	8.62
102	155	257	0.26	8.48	8.08		3		1	7.97
102	154	256	0.25	8.58	8.36					
102	153	255	0.26	8.43	8.72		1		−9	7.79
102	152	254	0.25	8.23	8.05					
102	151	253	0.25	8.41	8.01		−9		7	7.90
102	150	252	0.25	8.55	8.53					
102	149	251	0.25	8.75	8.73		7		5	8.48
101	157	258	0.26	7.27	7.09	−1	−11	7	3	6.80
101	156	257	0.26	7.56	7.49	−1		7		7.19
101	155	256	0.26		7.54	−1	3	7	1	7.13
101	154	255	0.26	7.91	7.79	−1		7		7.38
101	153	254	0.26		8.14	−1	1	7	−9	6.78
101	152	253	0.26	7.57	7.53	−1		7		6.99
101	151	252	0.26		7.50	−1	−9	7	7	6.82
101	150	251	0.25	7.96	8.05	−1		7		7.42
101	149	250	0.25		8.29	−1	7	7	5	7.37
101	148	249	0.25	8.44	8.54	−1		7		7.86
101	147	248	0.25		8.82	−1	5	7	1	7.87
101	146	247	0.25	8.76	8.81	−1		7		8.12
101	145	246	0.25	8.89	8.78	−1	1	7	−7	8.04

calculated with blocking for the Np isotopes are systematically overestimated. Calculations without blocking are clearly better for this isotopic chain. In uranium nuclei, both calculations agree well with the data for $N > 136$. For smaller N, there are quite large discrepancies. In the case of the model with blocking (but not the other one) these may come from discarding the reflection asymmetry.

To check the effect of the octupole deformation we have chosen the nucleus ^{225}U (see Fig. 1). We added deformations $\beta_{30}, \beta_{50}, \beta_{70}$ to the original grid and conducted the seven-dimensional minimization using the method with blocking. The reflection-asymmetric deformations of the found minimum were $\beta_{30} = 0.122, \beta_{50} = 0.045, \beta_{70} = 0.010$ and $\beta_{30} = 0.089, \beta_{50} = 0.043, \beta_{70} = 0.030$ in the parent and daughter nuclei, respectively. They reduce the g.s. energy by 0.6 MeV in the parent nucleus and by about 1.5 MeV in the daughter. This leads to the increase in α-decay energy by about 0.8 MeV, giving $Q_\alpha = 8.2$ MeV which agrees very well with the measured 8.00 MeV. Final results for ^{225}U (together with the corresponding results of the quasiparticle method) are summarized in Tables III and IV. It is likely that the results with blocking would improve also for some other neutron deficient nuclei.

For a set of 204 nuclei from the region of the fit one can compare the calculated and experimental Q_α values. The average deviation $\langle |Q_\alpha^{\exp} - Q_\alpha^{\text{th}}| \rangle$ amounts to 326 keV for the calculation with blocking and 225 keV for the quasiparticle method; the rms deviations are, respectively, 426 and 305 keV.

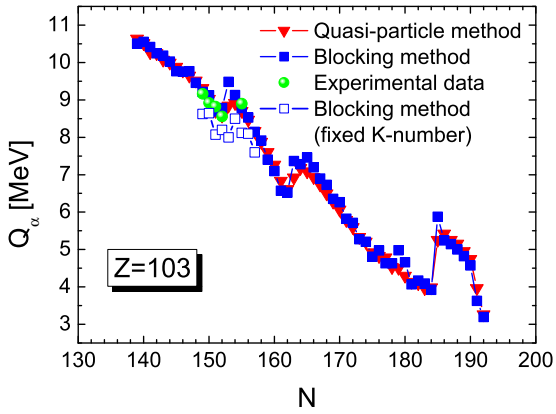

FIG. 4. (Color online) As in Fig. 1, but for Lr ($Z = 103$) isotopes. Additionally, transition energies to the parent g.s. configuration in daughter, calculated with blocking, are shown as open squares.

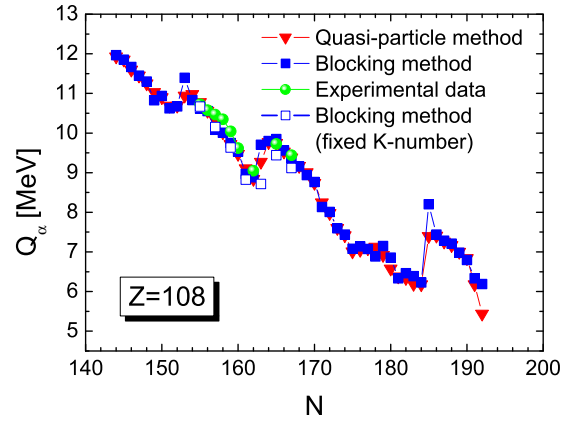

FIG. 6. (Color online) As in Fig. 4, but for Hs ($Z = 108$) isotopes.

Thus, the quasiparticle method gives a better agreement with experimental Q_α values in the region of the fit.

Starting with Fig. 3, we present the predictive part of the model: most of the masses of SH nuclei involved in α-decay energies were *not included* in the fit. The Q_α values calculated with blocking are compared to experimental data in Table V. We used mostly the data from [43], but in a few cases relied on other sources. In particular, the Q_α values in chains $^{293,294}117$ were based on [6,20] and deduced from the upper range of energies E_α when such a range exceeded the energy resolution of the detector (see Table II in [6]). The Q_α values are shown for a wider range of N in Fig. 3, separately for even- and odd-Z nuclei. In Figs. 4–7 the values calculated with and without blocking are shown vs experimental data for $Z = 103, 107, 108, 113$ nuclei. One should bear in mind that calculated decay energies *are independent* of the fitted energy shifts (average pairing energies), denoted h in Tables I and II.

The calculated Q_α vs N plots (Fig. 3) show a pronounced rise for N overstepping 184 and smaller ones at $N = 152$ and 162. They signal particularly well bound systems at these neutron numbers. The first one is connected with the magic spherical configuration (not yet tested by experiment) and the other two with the particularly stable prolate deformed configurations, corresponding to prominent gaps in the s.p. spectrum—see Fig. 10. One can notice that the maximum around $N = 162$ becomes wider for larger Z and some other maxima appear between $N = 160$ and 184, especially for $Z \geqslant 120$. On average, Q_α values increase with Z at constant N. A larger than average increase is predicted above $Z = 108$ for $N \leqslant 170$ and is related to the deformed proton subshell—see Fig. 10. It is visible in Fig. 3 as a larger gap between the plots for fixed Z, especially between $Z = 108$ and $Z = 110$. A number of smaller proton shell effects is predicted for limited ranges of N, like for $Z = 114$ around $N = 180$.

The rise in Q_α when going through $N = 152$ is supported by the data for $Z \geqslant 100$, but is much more gentle than the one calculated with blocking. A jump in Q_α across the closed "subshell" is much reduced in calculations without blocking, see Figs. 4–7. In the data, transition energy increases for at least two successive neutron numbers (this means for 153 and 154). The increase in Q_α above $N = 162$ is best seen in the data for Hs and Ds in Fig. 3, and roughly consistent with calculations; it is smaller than predicted for Rg. The proton shell effect at $Z = 108$ is seen in the data, but slightly smaller than calculated.

The Q_α values are reasonably well reproduced for $Z = 100$–106 nuclei, where they can be larger or smaller than the experimental ones. Decay energies are slightly

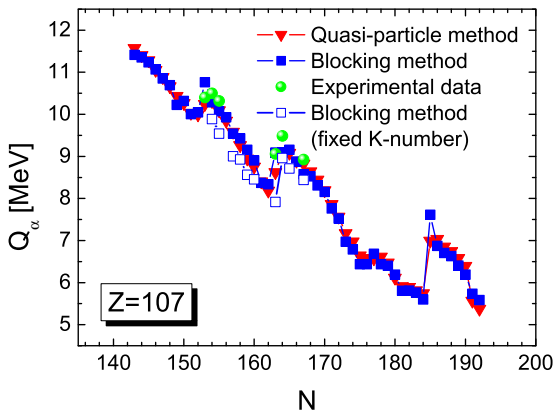

FIG. 5. (Color online) As in Fig. 4, but for Bh ($Z = 107$) isotopes.

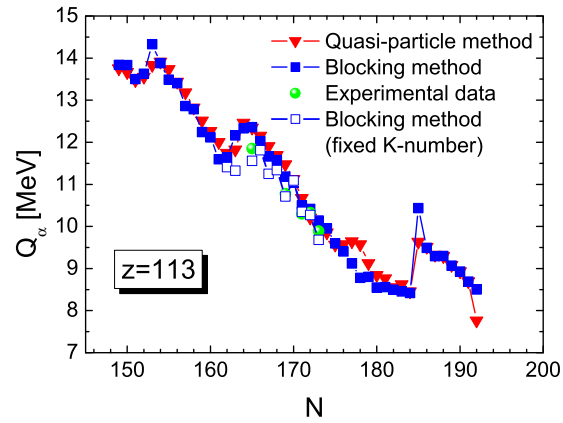

FIG. 7. (Color online) As in Fig. 4, but for $Z = 113$ isotopes.

underestimated for $Z = 108$ and systematically overestimated for $Z = 111,112,113$. For nuclei with $Z \geqslant 101$, the mean deviation $\langle|Q_\alpha^{\rm th} - Q_\alpha^{\rm exp}|\rangle$ and rms deviation are equal to, respectively, 217 keV and 274 keV in the calculation with blocking and 196 and 260 keV in the calculation with the quasiparticle method. Thus, both methods give similar deviations which are smaller than in the region of the fit. Among 88 experimental Q_α values in Table V, seven differ from the calculated ones by more than 0.5 MeV. In all cases the calculated values are too large. Five cases: ^{277,281}Cn, ^{279,280}Rg, and ^{266}Mt (the one with the largest deviation of 730 keV) signal the above-mentioned overestimation of Q_α which somehow tends to disappear for the heaviest known parent nuclei (see Table V). A similar overestimate results from the calculation without blocking. For two other cases, the $N = 153$ isotones of Rf and Sg (as well as of No, Db, and Bh), the calculation without blocking gives results consistent with the experimental values. Thus, these two cases, as well as results for other $N = 153$ isotones, should be understood as a specific failure of the calculation with blocking, described previously—the overshooting of the Q_α value just above the semimagic gap $N = 152$ (see Figs. 4–7). We have also checked the effect of a moderate 10% increase in the pairing strengths on the Q_α values within the method of blocking in the seven cases mentioned above. It turns out that such a change mostly lowers Q_α values by less than 100 keV and increases one of them by nearly 200 keV.

In trying to understand these results one has to remember that the g.s. to g.s. transitions are assumed in calculations. As mentioned in Sec. II, a predominance of transitions from the parent g.s. to an excited state in the daughter nucleus may result in attributing an apparent Q_α value lower than the true one. If one assumes that the α decay proceeds to the parent g.s. configuration in the daughter, one obtains energies shown in the last column in Table V. It may be seen that energies of these configuration-preserving transitions are reduced especially for particle numbers corresponding to one particle above a closed subshell. Predicted energies of configuration-preserving transitions are also shown in Figs. 4–7 for four isotope chains. A particularly large, about 2 MeV

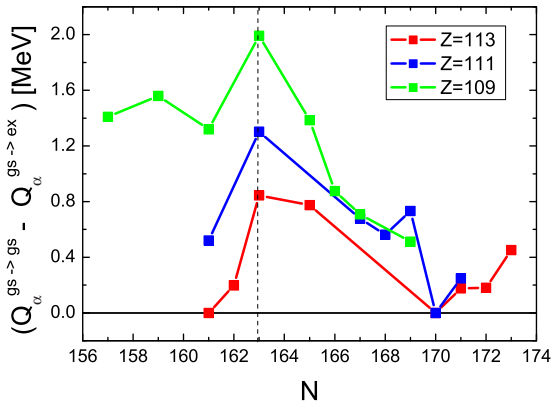

FIG. 8. (Color online) Excitation of the parent g.s. configuration in daughter nucleus calculated with blocking, equal to the predicted difference in transition energies, as a function of N for $Z = 109$, 111, 113.

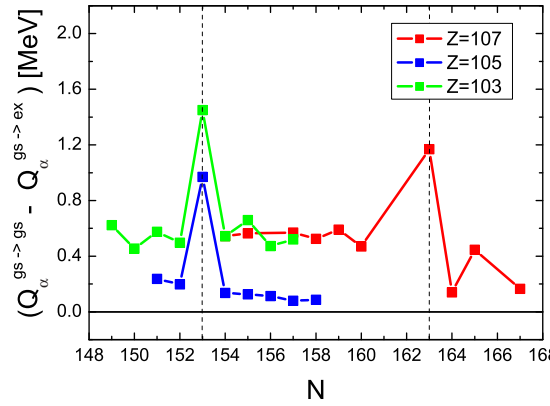

FIG. 9. (Color online) As in Fig. 8, but for $Z = 103$, 105, 107.

excitation of the parent configuration occurs in the daughter of ^{272}Mt; the excitation of about 1.5 MeV occurs for $Z = 103$, $N = 153$. These excitations, equal to the differences between g.s.→g.s. and configuration-preserving transition energies, $Q_\alpha^{\rm g.s.\ ->g.s.} - Q_\alpha^{\rm g.s.\ ->ex}$, are shown in Figs. 8 and 9. The particle numbers $Z = 103,109$ and $N = 153,163$ correspond to s.p. orbitals lying just above the large gaps.

This is illustrated in Fig. 10, where neutron and proton s.p. energies are shown vs β_{20}. The deformation β_{40} was

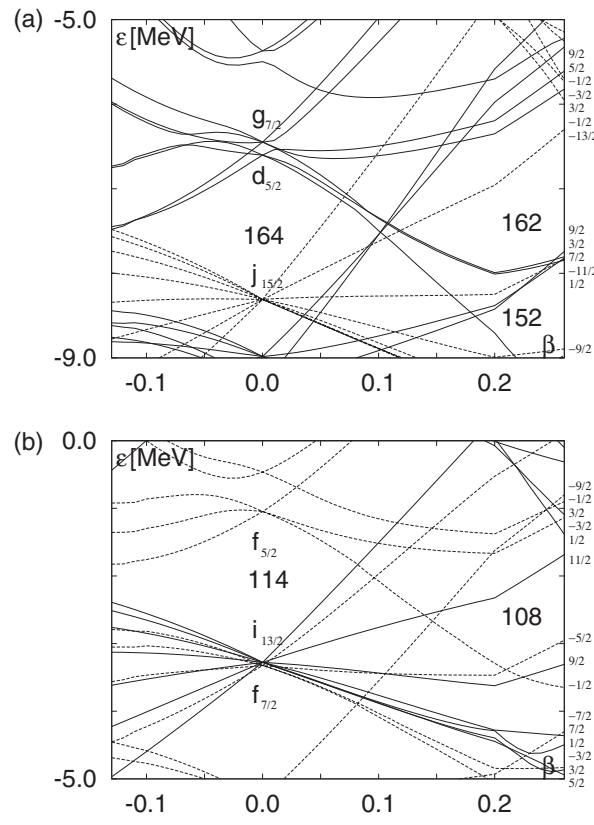

FIG. 10. Single-particle levels for neutrons (top) and protons (bottom) for $Z = 109$, $N = 163$. To roughly follow ground-state minima, deformation $\beta_{40} = 0$ for $\beta_{20} < 0$, then decreases linearly down to -0.08 at $\beta_{20} = 0.2$ and then linearly rises to -0.05 at $\beta_{20} = 0.26$. Positive (negative) parity levels are drawn with solid (dashed) lines; quantum numbers π, K are given to the right.

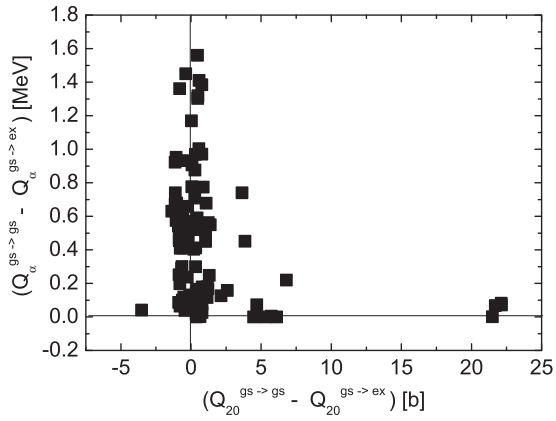

FIG. 11. Correlation between calculated parent-daughter deformation difference and the excitation of the parent g.s. configuration in daughter nucleus.

chosen to roughly follow g.s. minima around $Z = 109$, $N = 163$ ($\beta_2 = 0.22, \beta_4 = -0.08$): oblate minima for $Z \geqslant 115$ correspond to small β_4, prolate minima for $Z = 106, 107$ have $\beta_4 \approx -0.05$. As other deformations, differences in β_4 between isotopes and Z and N dependence are omitted, Fig. 10 can serve only a general orientation. It may be seen, that above $N = 162$ and $Z = 108$ the Woods-Saxon model predicts two intruder orbitals: neutron $K^\pi = 13/2^-$ and proton $11/2^+$. Similarly, the intruder neutron $K^\pi = 11/2^-$ and proton $9/2^+$ orbitals lie above $N = 152$, $Z = 102$. In general, such orbitals could combine spins and form a high-K isomer; for $Z = 109$, $N = 163$, our model predicts such a configuration as a ground state. A substantial hindrance of the g.s. to g.s. α decay could be expected in such case. Then, it is also not excluded that the g.s. decay would be so hindered, that the α decay would proceed from an excited state. Only future experimental data may show whether considering such a possibility will be necessary.

The predicted neutron and proton g.s. configurations are given in Table V, both for parent and daughter nuclei. They can be compared to the measured ones only in a few cases.

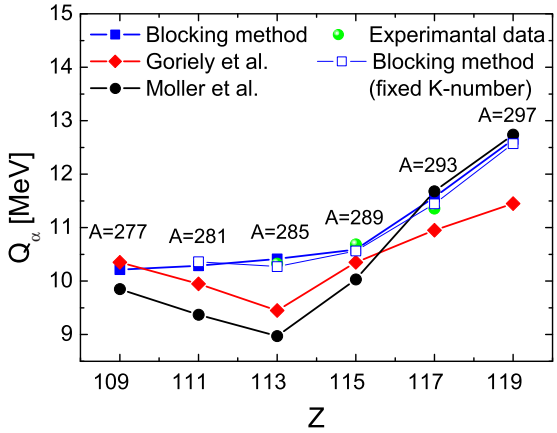

FIG. 12. (Color online) Q_α values in a chain beginning at a hypothetical nucleus $Z = 119$, $A = 297$, which contains the known chain for $^{273}117$—models vs experiment.

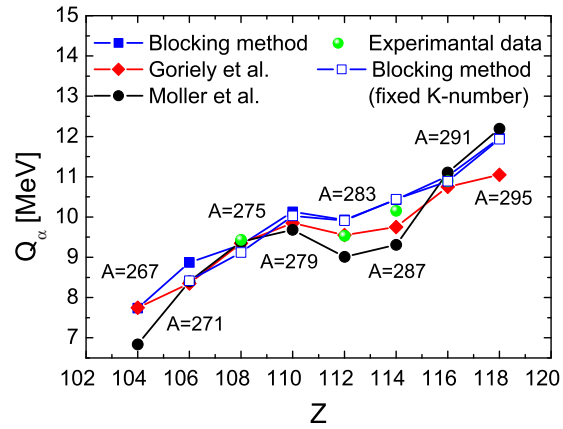

FIG. 13. (Color online) As in Fig. 12, but for $Z = 118$, $A = 295$.

For example, the $3/2^+$ g.s. of ^{257}No [45] is reproduced in our calculation. On the other hand, the predicted ground states in ^{255}Lr and ^{101}Md are interchanged with respect to the experimental results [46]. Ground state spins and parities evaluated from measurements in other Md, No, Lr, and Rf isotopes are consistent with our calculations, except for the measured or evaluated $7/2^-$ ground states in Md. The proton configurations predicted by the quasiparticle method are the same as in Table V. Mostly it is also the case for neutrons, except for the 155-th neutron being $1/2^+$ instead of $3/2^+$. The g.s. configurations in odd-A actinides, calculated within the Woods-Saxon model with the quasiparticle method, may be found in [19].

The g.s. to excited state transitions could also result from a deformation difference between parent and daughter. Such changes happen for some $Z \geqslant 114$ parent nuclei (weakly oblate to weakly prolate) and for parents with $Z = 111$–113, $N \approx 169$ (increase in prolate deformation). As can be seen in Fig. 11, the correlation between calculated deformation change and the excitation of the parent configuration in daughter is weak for nuclei investigated here: a large difference in quadrupole moments of the parent and daughter is not accompanied by a large change in the transition energy.

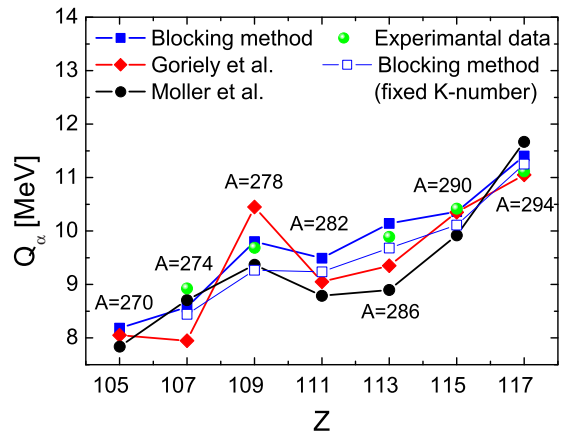

FIG. 14. (Color online) As in Fig. 12, but for $Z = 117$, $A = 294$.

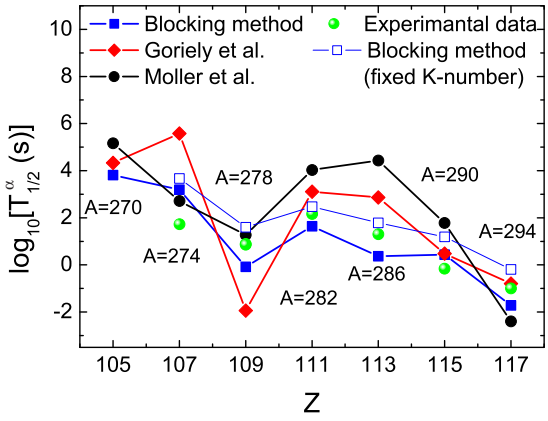

FIG. 15. (Color online) Calculated vs experimental α half-lives for the decay chain of $Z = 117$, $A = 294$.

The results of the model can also be appreciated by comparing successive transitions along the measured α decay chains. For the recently measured $^{294}117$ and $^{294}118$ chains [20] this is done in Figs. 13–15. The partially known decay chain for a hypothetical nucleus $^{297}119$ is shown in Fig. 12. The data were taken from [20,44] and some other sources [6,7].

After the successful synthesis of elements $Z = 117$ and $Z = 118$, the hypothetical nucleus $^{297}119$ is a natural candidate for the next synthesis experiment. One of the likely reactions leading to this element seems to be ^{48}Ca(^{252}Es,3n)$^{300-x}119$ see, e.g., [47]. Note, that this α-particle chain contains the known decay chain of $^{293}117$ [20]. One can see that our results reasonably agree with the experimental data and HFB-14 predictions [48]. However, for the nucleus $^{297}119$ our result is close to the model of Moller *et al.* [50], which underestimates Q_α values for lighter nuclides in the chain.

Another comparison is given in Fig. 13 for the α-particle chain starting at $^{295}118$. It may be seen that, compared to [50], a similar or better (especially for $^{283}112$ and $^{287}114$) agreement with the data is obtained by the present model. A similar conclusion follows when comparing the present results to the self-consistent calculations [48]. Note, that this α-particle chain contains the well-known chain of element $^{291}116$.

As an example of odd-odd systems, the alpha-chain for the nucleus $^{294}117$ is shown in Fig. 14. One may notice a good agreement between our Q_α values and the recently reported experimental data [6,20]. The other models deviate more from the measured Q_α values in this chain. This has an impact on the predicted alpha-decay lifetimes, as shown in Fig. 15. For example, in case of the HFB-14 approach [48], the half-life of ^{274}Bh is overestimated by four orders of magnitude while the one for ^{278}Mt is underestimated by three orders of magnitude. The half-lives resulting from [50] are systematically overestimated as a consequence of the underestimated Q_α values. (The Viola-Seaborg–type formula from [49] has been used to convert Q_α to half-lives). In all three discussed chains, our results are slightly overestimated. At present, however, the explanation that the allowed decays go to the excited states (lying slightly above the ground state), is not excluded, especially in the context of recent spectroscopic studies of element $Z = 115$ by Rudolph *et al.* [7].

IV. CONCLUSIONS

A systematic calculation of nuclear masses in the region of superheavy nuclei, including odd and odd-odd systems, was performed within the microscopic-macroscopic model with the Woods-Saxon deformed potential. Two versions of the model were used, with and without blocking. A fit in the region of heavy nuclei was performed to fix three additional parameters of the model, one for each group of odd-A and odd-odd nuclei, while keeping all previous parameters as they were used for even-even nuclei. Then, the Q_α values were calculated for SH nuclei as a prediction of the model to be compared against the data. The quality of the prediction turns out better than the quality of the model in the region of the fit: in the version with blocking, the mean and rms deviations of 217 and 274 keV for 88 SH nuclei are smaller than 326 and 426 keV for the 204 nuclei from the fit region. The quasiparticle method, clearly better in the region of the fit, for SH nuclei gives similar mean and rms deviations of 196 and 260 keV as the calculations with blocking.

Both versions of the model similarly overestimate Q_α values for $Z = 111$–113 and underestimate them, although to a lesser extent, around $Z = 107,108$. At present, these result should be treated with some care. Many of synthesized SH isotopes are odd-A or odd-odd nuclei and in many cases the statistics of E_α values is not large. Therefore it is not completely clear whether some of those cases may be explained by a hindrance of g.s. to g.s. transitions. The g.s. configurations of some SH nuclei, especially those involving high-K intruder orbitals, strongly hint to a possibility of α-decay hindrance, for example, for $Z = 109$, $N = 163$.

As comparisons to other models show, the agreement with data obtained here, without any parameter adjustment for Q_α and with a minimal adjustment for masses, is surely not worse. This gives a confidence that some refinements, especially in the treatment of pairing, may still moderately improve the agreement with data.

ACKNOWLEDGMENTS

This work was partially supported by Narodowe Centrum Nauki Grant No. 2011/01/B/ST2/05131. The support of the LEA COPIGAL fund is gratefully acknowledged.

[1] Yu. Ts. Oganessian *et al.*, Phys. Rev. Lett. **83**, 3154 (1999); Nature (London) **400**, 242 (1999); Phys. Rev. C **62**, 041604(R) (2000); **63**, 011301(R) (2001); **69**, 054607 (2004); Phys. Rev. Lett. **104**, 142502 (2010); Phys. Rev. C **74**, 044602 (2006); **79**, 024603 (2009).

[2] G. Münzenberg *et al.*, Z. Phys. A **300**, 1 (1981); **317**, 2 (1984); **309**, 1 (1982).

[3] S. Hofmann *et al.*, Z. Phys. A **350**, 4 (1995); S. Hofmann, Rep. Prog. Phys. **61**, 639 (1998); S. Hofmann *et al.*, Z. Phys. A **350**, 4 (1995); **354**, 1 (1996); Eur. Phys. J. A **48**, 62 (2012).

[4] Ch. E. Düllmann *et al*., Phys. Rev. Lett. **104**, 252701 (2010).
[5] L. Stavsetra, K. E. Gregorich, J. Dvorak, P. A. Ellison, I. Dragojevic, M. A. Garcia, and H. Nitsche, Phys. Rev. Lett. **103**, 132502 (2009).
[6] S. H. Liu *et al*., Phys. Rev. C **87**, 057302 (2013); Yu. Ts. Oganessian *et al*., *ibid*. **87**, 054621 (2013).
[7] D. Rudolph *et al*., Phys. Rev. Lett. **111**, 112502 (2013).
[8] S. Ćwiok, J. Dudek, W. Nazarewicz, J. Skalski, and T. Werner, Comput. Phys. Commun. **46**, 379 (1987).
[9] I. Muntian, Z. Patyk, and A. Sobiczewski, Acta Phys. Pol. B **32**, 691 (2001).
[10] M. Kowal, P. Jachimowicz, and A. Sobiczewski, Phys. Rev. C **82**, 014303 (2010).
[11] P. Jachimowicz, M. Kowal, and J. Skalski, Phys. Rev. C **85**, 034305 (2012).
[12] M. Kowal and J. Skalski, Phys. Rev. C **85**, 061302(R) (2012).
[13] P. Jachimowicz, M. Kowal, and J. Skalski, Phys. Rev. C **87**, 044308 (2013).
[14] M. Kowal and J. Skalski, Phys. Rev. C **82**, 054303 (2010).
[15] M. Kowal, P. Jachimowicz, and J. Skalski, arXiv:1203.5013 (2012).
[16] W. Brodziński and J. Skalski, Phys. Rev. C **88**, 044307 (2013).
[17] Z. Łojewski and A. Baran, Z. Phys. **329**, 161 (1988).
[18] S. Ćwiok, S. Hofmann, and W. Nazarewicz, Nucl. Phys. A **573**, 356 (1994).
[19] A. Parkhomenko and A. Sobiczewski, Acta Phys. Pol. B **35**, 2447 (2004); **36**, 3115 (2005).
[20] Yu. Ts. Oganessian *et al*., Phys. Rev. Lett. **109**, 162501 (2012).
[21] H. J. Krappe, J. R. Nix, and A. J. Sierk, Phys. Rev. C **20**, 992 (1979).
[22] G. Audi, O. Bersillon, J. Blachot, and A. H. Wapstra, Nucl. Phys. A **624**, 1 (1997).
[23] G. Audi, A. H. Wapstra, and C. Thobault, Nucl. Phys. A **729**, 337 (2003).
[24] F. Tondeur, S. Goriely, J. M. Pearson, and M. Onsi, Phys. Rev. C **62**, 024308 (2000); S. Goriely, M. Samyn, P. H. Heenen, J. M. Pearson, and F. Tondeur, *ibid*. **66**, 024326 (2002); S. Goriely, M. Samyn, M. Bender, and J. M. Pearson, *ibid*. **68**, 054325 (2003); M. Samyn, S. Goriely, M. Bender, and J. M. Pearson, *ibid*. **70**, 044309 (2004).
[25] L. W. Nordheim, Phys. Rev. **78**, 294 (1950).
[26] C. J. Gallagher and S. A. Moszkowski, Phys. Rev. **111**, 1282 (1958).
[27] A. K. Jain, R. K. Sheline, D. M. Headly, P. C. Sood, D. G. Burke, I. Hrivnacova, J. Kvasil, D. Nosek, and R. W. Hoff, Rev. Mod. Phys. **70**, 843 (1998).
[28] P. C. Sood, D. M. Headly, R. K. Sheline, and R. W. Hoff, At. Data Nucl. Data Tables **58**, 167 (1994).
[29] P. Möller, J. R. Nix, W. D. Myers, and W. J. Świątecki, At. Data Nucl. Data Tables **59**, 185 (1995).
[30] I. Ahmad *et al*., Phys. Rev. C **8**, 737 (1973).
[31] F. P. Hessberger, Eur. Phys. J. D **45**, 33 (2007).
[32] F. P. Hessberger *et al*., Eur. Phys. J. A **30**, 561 (2006).
[33] K. Abusaleem, Nucl. Data Sheets **112**, 2129 (2011).
[34] E. Browne and J. K. Tuli, Nucl. Data Sheets **114**, 1041 (2013).
[35] I. Ahmad *et al*., Phys. Rev. C **87**, 054328 (2013).
[36] S. Goriely, N. Chamel, and J. M. Pearson, Phys. Rev. C **82**, 035804 (2010).
[37] N. Chamel, A. F. Fantina, J. M. Pearson, and S. Goriely, Phys. Rev. C **84**, 062802(R) (2011).
[38] S. Goriely, M. Samyn, and J. M. Pearson, Phys. Rev. C **75**, 064312 (2007).
[39] S. Goriely, N. Chamel, and J. M. Pearson, Phys. Rev. C **88**, 024308 (2013).
[40] J. Duflo and A. P. Zuker, Phys. Rev. C **52**, R23 (1995).
[41] J. Duflo and A. P. Zuker (1996) (at htcsn-srv3.in2p3.fr/AMDC/theory)
[42] Min Liu, Ning Wang, Yangge Deng, and Xizhen Wu, Phys. Rev. C **84**, 014333 (2011).
[43] M. Wang, G. Audi, A. H. Wapstra, F. G. Kondev, M. MacCormick, X. Xu, and B. Pfeiffer, Chin. Phys. C **36**, 1603 (2012).
[44] M. Gupta and T. W. Burrows, Nucl. Data. Sheets **106**, 251 (2005); **107**, 789 (2006).
[45] M. Asai *et al*., Phys. Rev. Lett. **95**, 102502 (2005).
[46] A. Chatillon *et al*., Eur. Phys. J. A **30**, 397 (2006).
[47] K. Siwek-Wilczyńska, T. Cap, M. Kowal, A. Sobiczewski, and J. Wilczyński, Phys. Rev. C **86**, 014611 (2012).
[48] S. Goriely, F. Tondeur, and J. M. Pearson, At. Data Nucl. Data Tables **77**, 311 (2001).
[49] G. Royer, K. Zbiri, and C. Bonilla, Nucl. Phys. A **730**, 355 (2004).
[50] P. Moller, J. R. Nix, and K.-L. Kratz, At. Data Nucl. Data Tables **66**, 131 (1997).